Sputtering yields and surface chemical modification of tin-doped indium oxide in hydrocarbon-based plasma etching

Cite as: J. Vac. Sci. Technol. A **33**, 060606 (2015); https://doi.org/10.1116/1.4927125
Submitted: 11 May 2015 . Accepted: 08 July 2015 . Published Online: 23 July 2015

Hu Li, Kazuhiro Karahashi, Masanaga Fukasawa, Kazunori Nagahata, Tetsuya Tatsumi, and Satoshi Hamaguchi

Sputtering yields and surface chemical modification of tin-doped indium oxide in hydrocarbon-based plasma etching

Hu Li and Kazuhiro Karahashi
Center for Atomic and Molecular Technologies, Osaka University, Yamadaoka 2-1, Suita 565-0871, Japan

Masanaga Fukasawa, Kazunori Nagahata, and Tetsuya Tatsumi
Device and Material R&D Group, RDS Platform, Sony Corporation, Kanagawa 243-0014, Japan

Satoshi Hamaguchi[a)]
Center for Atomic and Molecular Technologies, Osaka University, Yamadaoka 2-1, Suita 565-0871, Japan

(Received 11 May 2015; accepted 8 July 2015; published 23 July 2015)

Sputtering yields and surface chemical compositions of tin-doped indium oxide (or indium tin oxide, ITO) by CH^+, CH_3^+, and inert-gas ion (He^+, Ne^+, and Ar^+) incidence have been obtained experimentally with the use of a mass-selected ion beam system and *in-situ* x-ray photoelectron spectroscopy. It has been found that etching of ITO is chemically enhanced by energetic incidence of hydrocarbon (CH_x^+) ions. At high incident energy incidence, it appears that carbon of incident ions predominantly reduce indium (In) of ITO and the ITO sputtering yields by CH^+ and CH_3^+ ions are found to be essentially equal. At lower incident energy (less than 500 eV or so), however, a hydrogen effect on ITO reduction is more pronounced and the ITO surface is more reduced by CH_3^+ ions than CH^+ ions. Although the surface is covered more with metallic In by low-energy incident CH_3^+ ions than CH^+ ions and metallic In is in general less resistant against physical sputtering than its oxide, the ITO sputtering yield by incident CH_3^+ ions is found to be lower than that by incident CH^+ ions in this energy range. A postulation to account for the relation between the observed sputtering yield and reduction of the ITO surface is also presented. The results presented here offer a better understanding of elementary surface reactions observed in reactive ion etching processes of ITO by hydrocarbon plasmas. © *2015 American Vacuum Society*.
[http://dx.doi.org/10.1116/1.4927125]

I. INTRODUCTION

Tin-doped indium oxide (or indium tin oxide, ITO) is a transparent conducting oxide (TCO), which has been widely used as transparent electrodes in various optoelectronic applications such as liquid crystal displays and solar panels due to its superior characteristics of electrical conductivity and optical transparency.[1,2] As the market demand for high-resolution optoelectronic devices such as head-mounted displays increases, technologies for micropattern formation by TCOs with a pattern resolution of submicrons or even nanometers are also highly demanded.

Surface patterning of ITO may be achieved by wet etching[3–5] or dry etching.[6–20] Reactive ion etching (RIE), which is a plasma-based dry etching technology, is especially suited for fine patterning of thin films. For RIE of ITO, halogen or hydrocarbon gases have been widely used as source gases for plasmas. Unlike halogen based gases, however, hydrocarbon gasses such as methane (CH_4) or methanol (CH_3OH) are noncorrosive and hydrocarbon-based plasmas are postulated to cause ion induced chemical reactions on ITO film surfaces to produce volatile metal organic compounds such as $In(CH_3)_3$ and $Sn(CH_3)_4$ (Refs. 7, 9, and 10) that may result in RIE of ITO. Such plasmas may also deposit carbon film on ITO.[18]

Whereas many earlier studies have examined various etching properties of ITO by hydrocarbon plasmas, the exact etching mechanisms of ITO, including surface chemical reactions between incident gaseous species and ITO, have been still unclear. In this study, therefore, as the first step toward a better understanding of the etching mechanisms of ITO by hydrocarbon plasmas, we attempt to clarify elementary surface interactions of ITO films with incident CH^+ and CH_3^+ ions with various incident energies.

II. EXPERIMENT

To examine interaction of incident CH_x^+ ions with an ITO sample surface, we have used a mass selected ion beam system, in which mass-selected ions with specific incident energy can be injected into a sample surface with a specified angle of incidence and the sample surface can be analyzed *in situ* by x-ray photoelectron spectroscopy (XPS). In the ion source of the system, a plasma is generated by arc discharge from a supplied gas. To generate hydrocarbon ions such as CH^+ and CH_3^+, we typically use a gas mixture of CH_4 and Ar for plasma generation. During the experiments of this study, the vacuum chamber was kept in an ultrahigh vacuum (UHV) condition with a pressure less than 10^{-8} Torr. More detailed information on this ion beam system may be found in Refs. 21–29.

A sample ITO, which contains about 3% of Sn, is a 2000 Å thick film on a 16 mm × 16 mm square silicon (Si) chip formed by sputtering deposition. Surface chemical compositions of an ITO sample set in the UHV reaction chamber of the beam system may be measured by XPS (using Mg $K\alpha$

a)Electronic mail: hamaguch@ppl.eng.osaka-u.ac.jp

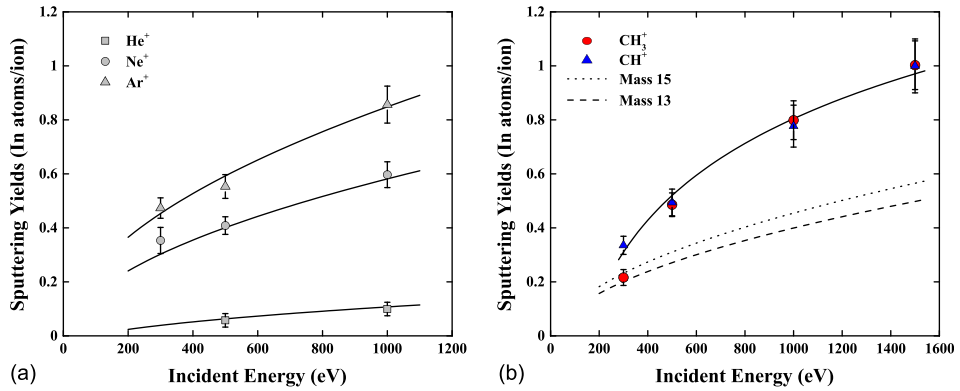

FIG. 1. (Color online) Sputtering yields of ITO by incident (a) He^+, Ne^+, and Ar^+, and (b) CH^+ or CH_3^+ ions, as functions of the incident ion energy. The solid curves represent fitting curves to observed sputtering yields. The functional form for the fitting curves is given by Eq. (A1). The dashed curves in Fig. 1(b) represent the estimated sputtering yield by ions of imaginary inert elements with atomic masses of 13 and 15 (which correspond to CH^+ and CH_3^+), obtained from the interpolation of the observed sputtering yields by He^+, Ne^+, and Ar^+ ions.

x-ray radiation) *in situ*, i.e., without being exposed to outside air.

The sputtering yield of ITO in this study is defined as the number of desorbed In atoms per incident ion. The sputtering yield reported in this study is derived from the etched depth of the ITO surface measured by a surface profiler (Dektak3ST) and the ion dose, which is estimated from the ion current and the beam irradiation time. The ion current is measured by a Faraday cup prior to each ion irradiation experiment.

III. RESULTS AND DISCUSSION

Figure 1 shows the sputtering yields of ITO by CH_3^+ and CH^+ ions as well as inert-gas ions, i.e., He^+, Ne^+, and Ar^+ ions, as functions of incident ion energy. As expected, the sputtering yield is an increasing function of the incident energy in each case. In Fig. 1(a), the solid curves represent fitting curves to observed sputtering yields of ITO by Ar^+, Ne^+, and He^+ ions, following the square-root dependence of the incident energy proposed by Steinbrüchel.[30] Using the known masses of Ar, Ne, and He atoms, we have interpolated the yield data by He^+, Ne^+, and Ar^+ ions given in Fig. 1(a) to obtain the sputtering yield curves by ions of imaginary inert elements with atomic masses of 13 and 15 (which correspond to CH^+ and CH_3^+), which are plotted by dashed curves in Fig. 1(b). A formula for the fitting curves as well as a method to obtain the physical sputtering yield of ITO by ions of an imaginary inert element with an arbitrary mass are given in the Appendix.

If there were no chemical reaction between incident CH^+ or CH_3^+ ions with the sample ITO surface (i.e., if the sputtering were purely physical), the ITO sputtering yield by CH^+ or CH_3^+ ions would be represented by the corresponding dashed curve as a function of the incident energy. In Fig. 1(b), the ITO sputtering yield by CH^+ or CH_3^+ ions is shown to be higher than the corresponding physical sputtering yield in general, especially when the incident energy is relatively high. The sputtering yields of Fig. 1(b) therefore indicate that the etching of ITO by CH^+ or CH_3^+ ions is chemically enhanced etching (i.e., RIE), especially in the high energy range.

It should be also noted that, in Fig. 1(b), the ITO sputtering yields by CH_3^+ and CH^+ ions take similar values when the incident energy is around 500 eV or higher. On the other hand, when the incident energy is lower, it is seen that the sputtering yield of ITO by CH_3^+ ions is lower than that by CH^+.

Figure 2 illustrates photoelectron spectra of the In ($3d_{5/2}$) and Sn ($3d_{5/2}$) core levels from *in-situ* XPS for ITO surfaces obtained after Ar^+ or CH_x^+ ion irradiation. Here, the background spectra were subtracted by the Shirley method and the Gaussian–Lorentzian functions with tail modifiers were used for curve fitting.[29] Prior to each beam experiment, the ITO sample surface was cleaned by 500 eV Ar^+ ions. It is seen that the XPS spectra of the initial ITO sample (prior to CH_x^+ ion injection) exhibits clear peaks for In-O and Sn-O bonds at 444.5 and 486.2 eV, which indicates that no metal is formed (i.e., no preferential sputtering of oxygen occurs) on the ITO surface by Ar^+ ion cleaning and the ITO consists of two separate phases of In_2O_3 and SnO_2.

In this study, a typical dose of CH^+ or CH_3^+ ions was in the range of (3–5) $\times 10^{16}$ ions/cm^2, at which the etching process reach steady state. It is seen that, after CH^+ or CH_3^+ ion injection, the spectra shifts toward the lower binding energy side, where new metallic bond peaks of In-In and Sn-Sn appear at 443.4 and 484.4 eV.

It is seen that, at 1000 eV incident energy, the both cases of CH^+ and CH_3^+ ion injections exhibit similar photoelectron spectra for In ($3d_{5/2}$) or Sn ($3d_{5/2}$) peak. However, at 300 eV, it is seen that the ITO surface becomes more metallic (i.e., more oxygen are preferentially desorbed) by CH_3^+ ions than CH^+ ions.

Percentages of different phases (i.e., metal and oxide phases) for In and Sn after ion beam injections are summarized in Table I. It is seen that, at 1000 eV irradiation by CH^+ or CH_3^+ ions, about a half of In_2O_3 loses its oxygen to form metal In on its surface whereas only about 20% of SnO_2 becomes metal Sn. In other words, oxygen of In_2O_3 is more preferentially sputtered than that of SnO_2. Indeed, it is

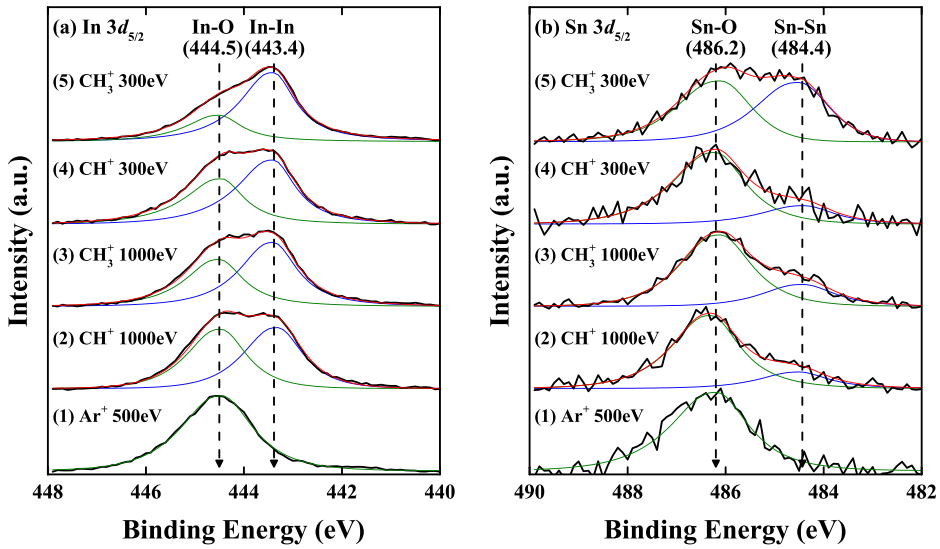

FIG. 2. (Color online) XPS spectra for (a) In $3d_{5/2}$ and (b) Sn $d_{5/2}$ of ITO surfaces after 500 eV Ar^+ ion cleaning, or CH^+ or CH_3^+ ion injection at 300 or 1000 eV.

known in earlier experiments[31,32] that SnO_2 is more congruently sputtered. These phenomena may be explained by the difference in bond strength between the In-O and Sn-O bonds; the bond energies of In-O and Sn-O are 346 and 528 kJ/mol.[33] As to the metallic phases, the bond energies of In-In and Sn-Sn are 82.0 and 187 kJ/mol.[33] Based on these bond energy values, we surmise that SnO_2 is more resistant against physical sputtering than In_2O_3 and the oxides are harder to etch physically than metal, as in the case of Ta.[29] Since the ITO film that we have examined in this study contains only a small amount of Sn, the sputtering yields of In_2O_3 by He^+, Ne^+, and Ar^+ are likely to be close to those given in Fig. 1. The sputtering yields of metallic In and Sn by inert gas ions are listed as functions of the incident energy in Refs. 34–36, which are higher than those of ITO given in Fig. 1 under the corresponding conditions. The sputtering yield data of ITO of this article and physical sputtering yields of In and Sn estimated in Refs. 35 and 36 are consistent with our surmise that the physical sputtering yields of metallic In and Sn are higher than those of In_2O_3 and SnO_2.

In the case of 300 eV injection of CH_3^+ ions, metallic components of In and Sn of ITO are shown to increase significantly; metallic Sn and In increase up to 50% and 70% in this case. In contrast, in the case of a 300 eV injection of CH^+ ions, the surface chemical states are essentially the same as those in the case of a 1000 eV injection of CH^+ or CH_3^+ ions. We have also confirmed by XPS that no carbon deposition occurred in any case examined in this study, even in the case of a 300 eV injection of CH^+ or CH_3^+ ions, although data are not shown here for the sake of brevity. These results indicate that, at low incident energy, the reduction of ITO is enhanced by the presence of hydrogen.

When the incident energy is sufficiently high (i.e., at 1000 eV in this study), the sputtering yields of ITO by CH^+ and CH_3^+ ions are nearly the same, as shown in Fig. 1, and the surface chemical compositions of the ITO sample surfaces are also nearly the same, as shown in Fig. 2. Since the masses of CH^+ and CH_3^+ ions are almost the same, physical sputtering effects by these two ionic species must be also almost the same. These facts indicate that the additional hydrogen supplied by the CH_3^+ ion beam has little additional chemical effects on the ITO surface. We postulate that C atoms of incident ions form CO and/or CO_2 molecules by reacting with O atoms of the ITO surface, which resulting in the depletion of oxygen and the formation of metallic In. Since the sputtering yield of metallic In is likely to be much higher than ITO, as we discussed above, the observed sputtering yield of ITO is significantly higher than its corresponding physical sputtering yield value, as shown in Fig. 1(b).

At lower incident energy below 500 eV, a chemical effect of hydrogen is more pronounced. In the case of CH_3^+ ion incidence, more metallic In and Sn are formed on the ITO surface. This may be understood because, at low incident energy, hydrogen atoms provided by the incident ions tend to remain near the top surface[24,26,37,38] and participate in the reduction of ITO on the surface. However, as we have observed in Fig. 1, despite the fact that more metallic In, which is considered to be less etch resistant, covers the sample surface, the sputtering yield by CH_3^+ ions is lower than that by CH^+ ions.

Although we do not know exactly why the ITO sputtering yield is lower with more incident hydrogen at low incident

TABLE I. Percentages of different phases (i.e., metal and oxide phases) for In and Sn after ion beam injections.

Component percentages (%)					
Ion species	Ar^+	CH^+	CH_3^+	CH^+	CH_3^+
Energy (eV)	500	1000	1000	300	300
In–In	0	51	58	59	72
In–O	100	49	42	41	28
Sn–Sn	0	18	23	20	49
Sn–O	100	82	77	80	51

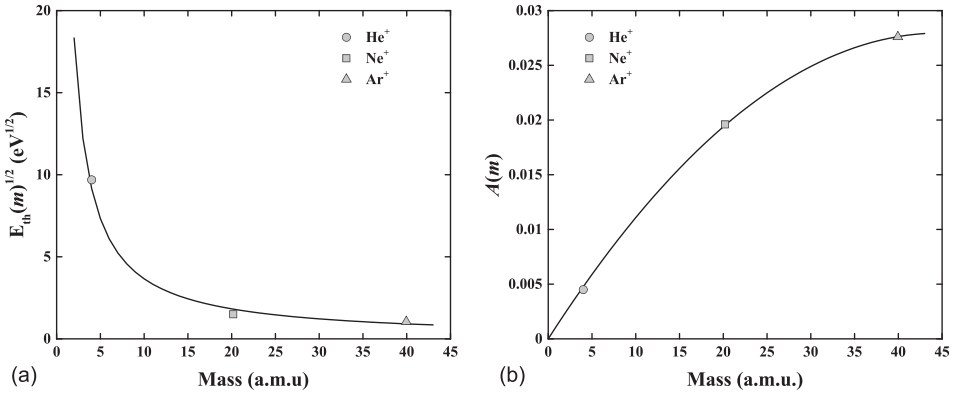

FIG. 3. Interpolated dependence of parameters $E_{th}^{1/2}$ and A of Eq. (A1) on the atomic mass m, obtained from the yield data for He^+, Ne^+, and Ar^+ ions given in Fig. 1(a).

energy, we postulate the following, based on an argument of energetics: When an incident hydrocarbon ion interacts with an ITO surface, part of its kinetic energy is used to reduce the ITO to form metallic In (and also Sn although the amount of Sn in the sample is small in this study) by carbon or hydrogen, which is an endothermic reaction [as the standard enthalpy of formation of In_2O_3 is -923 kJ/mol (Ref. 39)] and the remaining incident energy is used to sputter the surface material. In the case of low-energy incidence of CH_3^+ ions, more hydrogen is available on the ITO surface than in the case of CH^+ ions. Therefore, more reduction of ITO takes place and consequently less energy is available for sputtering of the surface material, which may result in the low sputtering yield in the case of CH_3^+ ion incidence observed in our beam study. At high incident energy (e.g., energy higher than 500 eV in Fig. 1), on the other hand, energy needed for reduction constitutes only a small portion of the total incident energy and therefore the difference in sputtering yield between the two cases of CH^+ and CH_3^+ is less pronounced. However, the mechanisms discussed above are just speculations and more detailed studies are required to clarify the mechanisms of ITO etching by incident hydrocarbon ions.

IV. SUMMARY AND CONCLUSIONS

We have examined sputtering yields and resulting changes in surface chemical composition for RIE of ITO by CH^+, CH_3^+, and inert gas ions (He^+, Ne^+, and Ar^+). It has been found that etching of ITO is chemically enhanced by energetic incidence of hydrocarbon (CH_x^+) ions. At high incident energy, the sputtering yields by CH^+ and CH_3^+ ions are equal, indicating that the contribution by hydrogen to the etching chemistry is not significant in this energy range. Furthermore, the ITO surface is partially reduced in a similar manner by either CH^+ or CH_3^+ ion incidence, so we expect that carbon of incident ions predominantly reduce In of the sample ITO by preferentially removing oxygen from In_2O_3 of the surface. However, at lower incident energy (less than 500 eV or so), a hydrogen effect on ITO reduction is more pronounced. The ITO surface is more reduced by CH_3^+ ions than CH^+ ions, resulting in the formation of more metallic In and Sn on the ITO surface. It has been observed that, under such low-energy incident conditions, the sputtering yield of ITO by CH_3^+ ions is lower than that by CH^+ ions despite the fact that incident CH_3^+ ions reduce ITO more than CH^+ ions, covering the surface with more metallic In, which is typically less resistant against physical sputtering. The results presented here offer a better understanding of elementary surface reactions observed in RIE processes of ITO by hydrocarbon plasmas.

APPENDIX

In this Appendix, a formula for the physical sputtering yield of ITO by ions of an imaginary inert element with an arbitrary mass is proposed as a function of the ion incident energy. The yield should agree with the actual physical sputtering yield by inert gas ions such as He^+, Ne^+, and Ar^+ if the incident ions are such actual ions. Following Steinbrüchel,[30] we propose that the physical sputtering yield Y of ITO by ions of an inert element with mass m is given by the following formula;

$$Y = A(m)(E^{1/2} - E_{th}(m)^{1/2}), \tag{A1}$$

where E is the ion incident energy, A is a proportional constant, and E_{th} represents the threshold energy. The parameters A and E_{th} depend on the mass m in general, especially for elements lighter than Ar.[40,41] The solid curves of Fig. 1(a) follow the formula above, from which we obtain the values of $A(m)$ and $E_{th}(m)$ for m = 4 (for He), 20 (Ne), and 40 (Ar). The interpolated functions $A(m)$ and $E_{th}(m)$ for an imaginary inert element with mass m in the range of $4 \leq m \leq 40$ that we have used in this study are given in Fig. 3 and Table II.

TABLE II. Fitting formulae with their parameter values for $E_{th}^{1/2}$ and A of Eq. (A1) as functions of the atomic mass m.

Formula	$E_{th}(m)^{1/2}$ am^b	A(m) $am^2 + bm$
a	36.68	-1.39×10^{-5}
b	−1.00	1.25×10^{-3}

[1]K. L. Chopra, S. Major, and D. K. Pandya, Thin Solid Films **102**, 1 (1983).
[2]M. Venkatesan, S. McGee, and U. Mitra, Thin Solid Films **170**, 151 (1989).
[3]G. Bradshaw and A. J. Hughes, Thin Solid Films **33**, L5 (1976).
[4]Z. Calahorra, E. Minami, R. M. White, and R. S. Muller, J. Electrochem. Soc. **136**, 1839 (1989).
[5]T. Ratcheva and M. Nanova, Thin Solid Films **141**, L87 (1986).
[6]T. Minami, T. Miyata, A. Iwamoto, S. Takata, and H. Nanto, Jpn. J. Appl. Phys., Part 2 **27**, L1753 (1988).
[7]M. Mohri, H. Kakinuma, M. Sakamoto, and H. Sawai, Jpn. J. Appl. Phys., Part 2 **29**, L1932 (1990).
[8]I. Adesida, D. G. Ballegeer, J. W. Seo, A. Ketterson, H. Chang, K. Y. Cheng, and T. Gessert, J. Vac. Sci. Technol., B **9**, 3551 (1991).
[9]R. J. Saia, R. F. Kwasnick, and C. Y. Wei, J. Electrochem. Soc. **138**, 493 (1991).
[10]H. Sakaue, M. Koto, and Y. Horiike, Jpn. J. Appl. Phys., Part 1 **31**, 2006 (1992).
[11]L. Y. Tsou, J. Electrochem. Soc. **140**, 2965 (1993).
[12]K. Nakamura, T. Imura, H. Sugai, M. Ohkubo, and K. Ichihara, Jpn. J. Appl. Phys., Part 1 **33**, 4438 (1994).
[13]J. Molloy, P. Maguire, S. J. Laverty, and J. A. McLaughlin, J. Electrochem. Soc. **142**, 4285 (1995).
[14]M. Takabatake, Y. Wakui, and N. Konishi, J. Electrochem. Soc. **142**, 2470 (1995).
[15]Y. Kuo, Jpn. J. Appl. Phys., Part 2 **36**, L629 (1997).
[16]Y. Kuo and T. L. Tai, J. Electrochem. Soc. **145**, 4313 (1998).
[17]Y. J. Lee, J. W. Bae, H. R. Han, J. S. Kim, and G. Y. Yeom, Thin Solid Films **383**, 281 (2001).
[18]D. Y. Kim, J. H. Ko, M. S. Park, and N. E. Lee, Thin Solid Films **516**, 3512 (2008).
[19]S. I. Kim and K. H. Kwon, Trans. Electr. Electron. Mater.**10**, 1 (2009).
[20]S. Major, S. Kumar, M. Bhatnagar, and K. L. Chopra, Appl. Phys. Lett. **49**, 394 (1986).
[21]K. Ishikawa, K. Karahashi, H. Tsuboi, K. Yanai, and M. Nakamura, J. Vac. Sci. Technol., A **21**, L1 (2003).
[22]K. Karahashi, K. Yanai, K. Ishikawa, H. Tsuboi, K. Kurihara, and M. Nakamura, J. Vac. Sci. Technol., A **22**, 1166 (2004).
[23]K. Yanai, K. Karahashi, K. Ishikawa, and M. Nakamura, J. Appl. Phys. **97**, 053302 (2005).
[24]T. Ito, K. Karahashi, M. Fukasawa, T. Tatsumi, and S. Hamaguchi, Jpn. J. Appl. Phys., Part 1 **50**, 08KD02 (2011).
[25]T. Ito, K. Karahashi, M. Fukasawa, T. Tatsumi, and S. Hamaguchi, J. Vac. Sci. Technol., A **29**, 050601 (2011).
[26]T. Ito, K. Karahashi, K. Mizotani, M. Isobe, S.-Y. Kang, M. Honda, and S. Hamaguchi, Jpn. J. Appl. Phys., Part 1 **51**, 08HB01 (2012).
[27]T. Ito, K. Karahashi, S.-Y. Kang, and S. Hamaguchi, J. Vac. Sci. Technol., A **31**, 031301 (2013).
[28]K. Karahashi and S. Hamaguchi, J. Phys. D: Appl. Phys. **47**, 224008 (2014).
[29]H. Li, Y. Muraki, K. Karahashi, and S. Hamaguchi, J. Vac. Sci. Technol., A **33**, 040602 (2015).
[30]C. Steinbrüchel, Appl. Phys. Lett. **55**, 1960 (1989).
[31]K. S. Kim, W. E. Baitinger, J. W. Amy, and N. Winograd, J. Electron Spectrosc. **5**, 351 (1974).
[32]R. Kelly, Nucl. Instrum. Methods **149**, 553 (1978).
[33]*CRC Handbook of Chemistry and Physics*, 91st ed., edited by W. M. Haynes (Taylor & Francis, Boca Raton, FL, 2010).
[34]R. C. Krutenat and C. Panzera, J. Appl. Phys. **41**, 4953 (1970).
[35]Y. Yamamura and H. Tawara, At. Data Nucl. Data Tables **62**, 149 (1996).
[36]*Sputtering by Particle Bombardment: Experiments and Computer Calculations from Threshold to MeV Energies*, Topics in Applied Physics, edited by R. Behrisch and W. Eckstein (Springer, New York, 2007), Vol. 110.
[37]K. Mizotani, M. Isobe, M. Fukasawa, K. Nagahata, T. Tatsumi, and S. Hamaguchi, J. Phys. D: Appl. Phys. **48**, 152002 (2015).
[38]K. Mizotani, M. Isobe, and S. Hamaguchi, J. Vac. Sci. Technol., A **33**, 021313 (2015).
[39]E. H. P. Cordfunke, R. J. M. Konings, and W. Ouweltjes, J. Chem. Thermodyn. **23**, 451 (1991).
[40]N. Laegreid and G. K. Wehner, J. Appl. Phys. **32**, 365 (1961).
[41]D. Rosenberg and G. K. Wehner, J. Appl. Phys. **33**, 1842 (1962).